FDTD simulation study of size/gap and substrate-dependent SERS activity study of Au@SiO_2 nanoparticles*

Jing-Liang Yang(杨晶亮), Ruo-Ping Li(李若平), Jun-He Han(韩俊鹤), and Ming-Ju Huang(黄明举)†

Key Laboratory of Informational Opto-Electronical Materials and Apparatus, School of Physics and Electronics, Henan University, Kaifeng 475004, *China*

(Received 19 November 2015; revised manuscript received 19 April 2016; published online 25 June 2016)

We use Au@SiO_2 nanoparticles (NPs) to systematically and comprehensively study the relationship between nanostructure and activity for surface-enhanced Raman scattering. Calculation simulation using the finite different time domain method verifies the experiment results and further reveals that the particle size and the distance between the NPs play vital roles in the surface-enhanced Raman scattering (SERS). Furthermore, in order to better simulate the real experiment, a Au@SiO_2 nanosphere dimer is placed on the silicon substrate and Au substrate, separately. The simulation results show that the large EM field coupling is due to the "hot spots" transferred from the NP–NP gaps to NP–surface of metal gaps, meanwhile, more "hot spots" occur. We also find that the signal intensity strongly depends on the position of the probe molecule. This work provides a better understanding of EM field enhancement.

Keywords: Au@SiO_2 NPs, FDTD, SERS, EM coupling

PACS: 33.20.Fb, 47.54.Bd, 47.54.Jk, 52.38.–r **DOI:** 10.1088/1674-1056/25/8/083301

1. Introduction

The Raman scattering from pyridine molecules adsorbed on a silver electrode surface can increase a million times or more as great as the signal from the free molecules. This is known as surface-enhanced Raman scattering (SERS).[1] Because it has high detection sensitivity, SERS technique has been widely applied to food safety,[2] electrochemistry,[3] and other fields.[4] As currently understood, SERS enhancement mode mainly includes electromagnetic (EM) coupling enhancement and chemical enhancement (CE).[5–8] The EM mechanism describes the enhanced local EM fields due to resonant excitation of plasma in the metallic nanostructure surface.[9,10] This purely physical effect is by far the most dominant contribution, with standard SERS enhancement factors (EFs) in a wide range of 10^3–10^{10}. CE, only two–three orders of magnitude, is significantly smaller than the contribution of the EM coupling enhancement.[11] But how to validate the relationship between nanostructures and EM coupling is still a significant challenge in experiment.

Tip-enhanced Raman spectroscopy (TERS) was invented in 2000 — the pure Ag or Au or their coated atomic force microscope (AFM) tip acts as an antenna for both incident and Raman field.[12–14] If the substrate is metallic, the great EM field appears at the junction between the tip and substrate. This gap-mode can obtain much stronger Raman signal than normal SERS. It can even realize a single molecular detection limit for some resonant molecules.[15,16] However, there are some inherent defects. Firstly, for non-metallic surfaces there is no EM coupling between the tip and the substrate surface, the Raman signal of TERS is still too low to detect molecules. Secondly, the molecules in solution may be adsorbed on the tip and pollute the tip. Thirdly, the TERS instrument is too complicated and too expensive for practical application. In the market or human life, or other more practical applications, the material should be universal and available. This means that the signal should have good reproducibility. Meanwhile, the technique should be easily handled and cost-effective. The key advances made by shell-isolated nanoparticle-enhanced Raman spectroscopy (SHINERS) are a tremendous expansion of SERS versatility and much higher detection sensitivity than TERS.[17–19] In addition, SHIN can avoid the charge-transfer effect, therefore, the signal is more reliable and more stable. Precise control of the SiO_2 shell thickness can bring convenience to study the EM coupling between the interparticle spacing.

The size, morphology, and interparticle spacing of the nanoparticles (NPs) are very important in the SERS, so a lot of research work mainly focused on using photoetching method to study the surface morphology, particle size and the interparticle spacing for SERS.[20,21] However, the high cost of sample prepared method hinders practical application. Therefore, we use the simple and feasible method through adjusting the shell thickness on the surface of NPs to study the particle size and interparticle spacing in the SERS here, in order to systematically understand the EM coupling effect relationship between the particle size and gap. Experimentally, Au@SiO_2 NPs with 2-nm–3-nm shell thickness, and ca. 15-nm, 25-nm, 50-nm core sizes were prepared, respectively. Meanwhile, Au@SiO_2 NPs with 25-nm core size, and ca. 3-nm, 15-nm, 35-nm, 50-nm shell thicknesses were prepared. A Au@SiO_2 nanosphere dimer was chosen to simulate the experiment and

*Project supported by the National Natural Science Foundation of China (Grant No. 61177004).

†Corresponding author. E-mail: mingjuh@163.com

© 2016 Chinese Physical Society and IOP Publishing Ltd

calculate the EM field distribution by the finite different time domain (FDTD) method. Furthermore, in order to better simulate the real experiment, a Au@SiO_2 nanosphere dimer was placed on the silicon substrate and Au substrate, separately. The simulation results show that the large EM field coupling is due to the "hot spots" transferred from the NP–NP gaps to NP–surface of metal gaps, meanwhile, more "hot spots" occur. The FDTD calculation results accord well with the experimental data. The findings in this work can guide us in designing the metallic nanostructures to obtain the strongest EM coupling enhancement.

2. Experiment

2.1. Preparation of gold NPs

Gold sol was prepared by the Frens method.[22] 100 ml of 0.01-wt% aqueous solution of $HAuCl_4$ was placed in a round-bottom flask and heated to boiling under stirring. Next, 1 ml of 0.25-mM trisodium citrate solution was added quickly into the boiling solution, and the mixture was kept boiling gently for 30 min with continuous stirring. Then, the solution was cooled to the room temperature and put in a dark place before further use. By changing the amount of trisodium citrate which was added, to obtain different sizes of gold NPs, the sizes of 15 nm, 25 nm, and 50 nm of gold NPs were prepared.

2.2. Preparation of Au@SiO_2 NPs

For coating gold NPs with amorphous silica shells, two methods to prepare Au@SiO_2 NPs were used. The first method according to classic Stober method:[23] 8-ml gold sol was dissolved in 20-ml isopropanol, and stirred for 3 min–5 min. Next, 0.5-ml aqueous ammonia was added rapidly, and then 5 μl of tetraethylorthosilicate (TEOS) was added, then stirred for 3 h. Different shell thickness can be obtained by controlling the reaction time and adding a certain amount of TEOS. With this method, we obtained Au NPs ($\sim$ 25 nm) coated with SiO_2 shell of thickness ca. 15 nm, 35 nm, and 50 nm, respectively.

The second method is presented by Li *et al.*,[17] 0.4 ml of 1-mM aqueous solution of (3-aminopropyl)trimethoxysilane (APTMS) was added to 30 ml of gold sol and stirred at 25 °C for 15 min. Subsequently, 3.2 ml of freshly prepared diluted sodium silicate solution (0.54 wt% of SiO_2) adjusted with HCl to PH 9.6–PH 11 was added with stirring 3 min–5 min. Then, we placed the flask in a 90-°C water bath and stirred the contents for 10 min–60 min. After the reaction finished, the flask was placed in ice–water mixture to terminate the reaction quickly.

2.3. Preparation of Au@SiO_2 NPs monolayer film

Au@SiO_2 NPs monolayer film was prepared according to Li's method.[24] 5 ml of cyclohexane was added in 15-ml Au@SiO_2 NPs colloid. Then 4 ml of ethanol was added with stirring 3 min–5 min. Then, cyclohexane was removed with a glue dropper head. The Au@SiO_2 NPs monolayer film was transferred onto gold film and silicon for further experiments. The scanning electron microscopy (SEM) images are shown in the Supporting Information (S1 and S2).

2.4. Preparation of Au@SiO_2 NPs film with absorbed molecules

The gold film and silicon were purchased from German Tech Co., Ltd and Henghao Industrail, respectively. The average roughness of gold film was less than 3 nm. Prior to use, the gold film and silicon wafer were immersed in a mixture of concentrated sulfuric acid and hydrogen peroxide for 15 min, then rinsed by water and dried with nitrogen. The clean gold film and silicon were immersed in 10^{-6} mol/L R6G solution for 1 h–2 h and then rinsed with ethanol. After drying, the Au@SiO_2 NPs monolayer film was transferred onto it.

3. Results and discussion

3.1. Effect of Au NPs' size on the SERS signal

Experimentally, it is difficult to precisely control the distance between the Au NPs. In addition, the Raman signal will

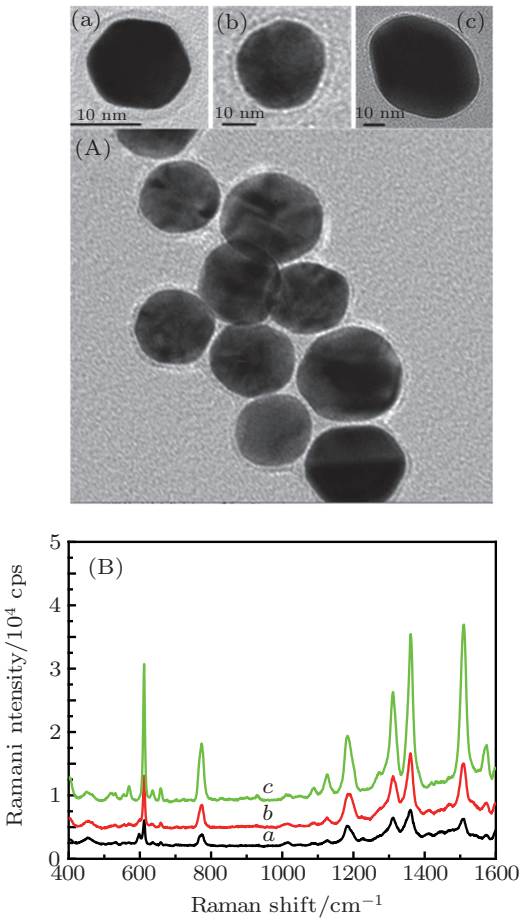


Fig. 1. (color online) TEM images of Au@SiO_2 NPs with core sizes of (curve *a*) 15 nm, (curve *b*) 25 nm, and (curve *c*) 50 nm, and corresponding SERS spectra of Rh6G molecule adsorbed in the gap between Au@SiO_2 NPs. Laser: 632.8 nm, 20 mW.

be distorted when the probe molecules directly contact bore Au NPs. Therefore, In order to analyze the effect of core size on the SERS signal, Au@SiO_2 NPs with 2 nm–3 nm in shell thickness, and ca. 15-nm, 25-nm, and 50-nm core sizes are prepared, respectively, the transmission electron microscopy (TEM) images are shown in Fig. 1(A). Then a monolayer film of Au@SiO_2 NPs was deposited on the silicon substrate surface after rinsing with ethanol (see the previous section). Figure 1(B) shows the SERS spectra (laser: 632.8 nm, 20 mW) of R6G with different core sizes of Au@SiO_2 NPs. Encouragingly, the SERS signal of R6G molecules adsorbed at the gap between Au@SiO_2 NPs (with $\sim$ 50 nm core/shell 2 nm–3 nm) exhibits a notable Raman enhancement. The enhancement signal is much higher than those of R6G molecules adsorbed at the gap between Au@SiO_2 NPs (core size 15 nm) and (core size 25 nm) referred to as spectra (curve *a*) and (curve *b*). It is apparent that the SERS signal intensity is attributed to the increase of the particle size.

3.2. Effect of the Au@SiO_2 NPs silica shell thickness on the SERS signal

In our experiment, the Au NPs with 25-nm average diameter have much better monodispersity. In order to verify the effect of the interparticle spacing on the same particle size, the Au@SiO_2 NPs with core size 25 nm and different thicknesses are prepared as shown in Fig. 2(A) and Fig. S1. For a monolayer film of Au@SiO_2 NPs prepared by the above method, its Raman spectra (laser: 632.8 nm, 20 mW) are shown in Fig. 2(B). When comparing the samples, the SERS signal of R6G molecules adsorbed at the gap between Au@SiO_2 NPs (shell thickness 2 nm–3 nm), referring to spectrum (curve *d*), shows the largest enhancement. The enhancement signal is much greater than those of R6G molecules adsorbed at the gaps between Au@SiO_2 NPs with a shell thickness of 15 nm and those with shell thickness 35 nm, referring to spectra (curve *c*) and (curve *b*). However, for Au@SiO_2 NPs with a shell thickness of 50 nm, the enhancement signal still exists, which shows that a long tail effect occurs in the induced EM field,[20] referring to spectrum (curve *a*) and the peaks in Fig. S5.

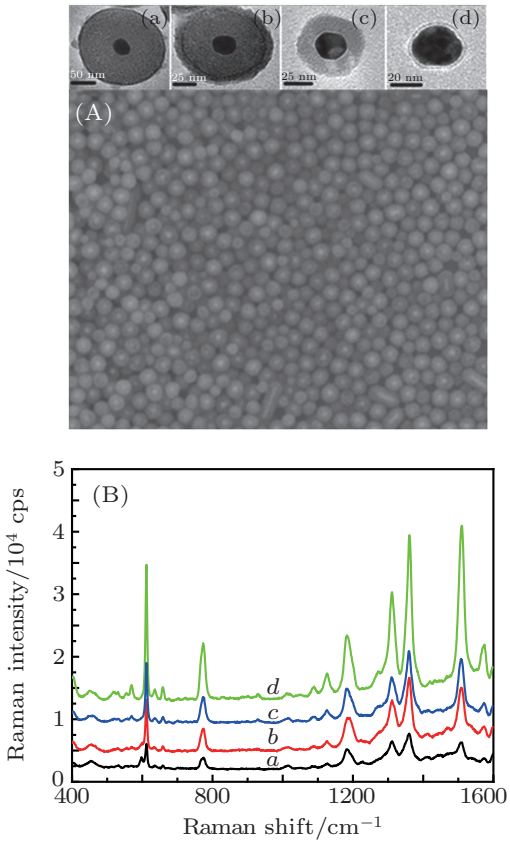


Fig. 2. (color online) SEM images of Au@SiO_2 NPs with shell thickness of (a) 50 nm, (b) 35 nm, (c) 15 nm, and (d) 3 nm, and corresponding SERS spectra of Rh6G molecule adsorbed in the gap between Au@SiO_2 NPs. Laser: 632.8 nm, 20 mW.

3.3. FDTD simulation of the EM field distribution of Au@SiO_2 NPs dimer

In the coupled NP system, an Au@SiO_2 nanosphere dimer is chosen to simulate the above SERS experiment and calculate the EM field distribution by the finite different time domain (FDTD) method. The calculation results show that the particles' size and the distance between the NPs play vital roles in the Raman signal enhancement. As shown in Figs. 3(a)–3(c) and Fig. S3, where the 633-nm laser is used to simulate calculation, with the diameter of Au@SiO_2 NPs fixed to be 50 nm, the smaller the gap size of Au@SiO_2 NPs dimer is, the larger the maximum EM coupling intensity reaches. The reason is that the aggregation occurs because the NPs are very close to each other, and the absorption wavelength of the NPs is changed accordingly. When the absorption wavelength of the aggregated NPs is the same as the laser wavelength, the surface plasma resonance (SPR) strength will increase significantly, meanwhile, EM field coupling intensity becomes stronger. In addition, as shown in Figs. 3(b) and 3(c), and Fig. S4, when the gap is 4 nm, the EM field intensity is attributed to the increase of the particle size. Because the SPR is related to the charge density, the larger the size of Au NPs, the more free electrons on the surface of Au NPs and the stronger the SPR becomes, meanwhile, EM coupling becomes stronger. Moreover, the SPR peaks of the Au NPs are red-shifted obviously with NPs size increasing, and the size is larger, the red shift is more obvious. The appropriate laser wavelength will cause a stronger SPR between the large Au NPs dimers. Ultimately, we reach the conclusion that the larger the particle size and the narrower the gap, the stronger the EM field coupling intensity is. The results show that theoretical calculations are in good agreement with the experimental results.

Actually, very strong EM field is only observed in "hot spots" in junctions between two particles. As is well known, the maximum EM field is tightly confined near the NPs surface. Only the molecules which are absorbed on or very close

to the gap can have a giant enhancement from SERS. The signal enhancement is determined by the NP size, the gap, and the position of the probe molecules in the "hot spots". In addition, only the averaged surface enhancement factor (ASEF) can veritably and fully reflect the overall enhancement of the substrate. A simple calculation is offered to explain ASEF, only a few molecules (ca. 2%) in "hot spots" contribute to 98% of the total Raman signals, the average of all molecules Raman signal from the nanoparticle surface is still weak. How to obtain the strongest Raman signal and much more "hot spots" in the metallic nanostructures is still an enormous challenge in experiment.

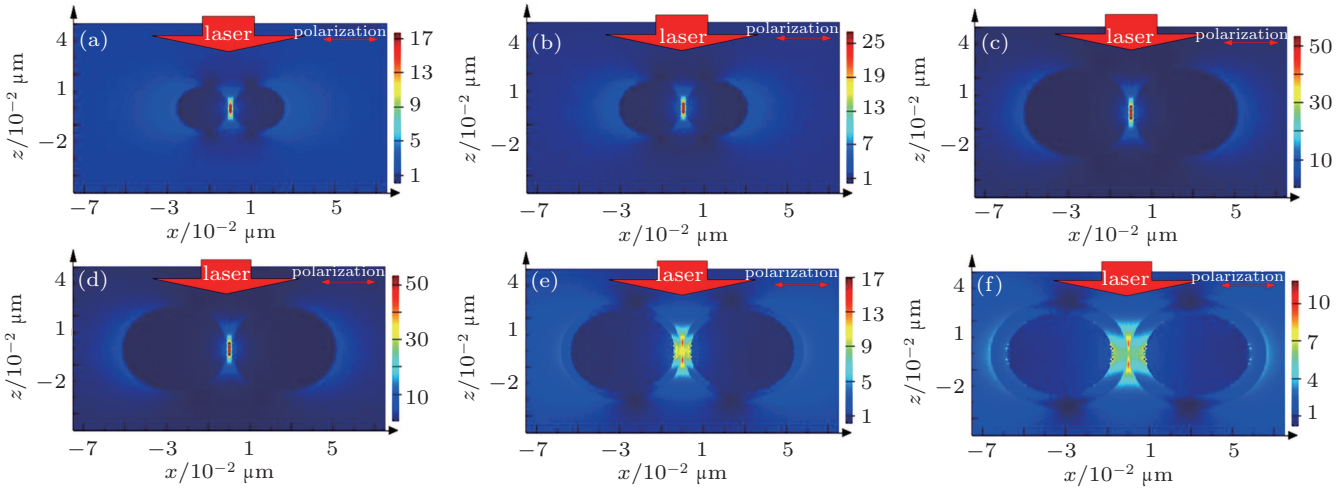


Fig. 3. (color online) EM field distributions of Au@SiO_2 dimer, simulated by FDTD method. Directions of incidence and polarization of the 633-nm excitation laser are shown in the figure. The thickness of the silica shell is 2 nm, and the diameters of Au@SiO_2 NPs are (a) 15 nm, (b) 25 nm, and (c) 50 nm. The diameter of the Au core is 25 nm, the thickness values of the silica shell are (d) 2 nm, (e) 4 nm, and (f) 8 nm.

3.4. FDTD simulation of a Au@SiO_2 NP dimer on different substrates

In practice, glass sheets and silicon wafers are widely used as the supports of metal NPs. The FDTD method is used to simulate the EM field distribution of the Au@SiO_2 NPs on different substrates (parameters: diameter $d_{Au} = 50$ nm, shell thickness = 2 nm, $\lambda = 633$ nm). As shown in Fig. 4(a), for the Au@SiO_2 NPs dimer on silicon wafer, the presence of a dielectric material (silicon) around the NPs will lead to a shift of SPR peaks of metal NPs, but will not cause an obvious change of the EM field distribution.[21] However, if a metal substrate is used, as shown in Fig. 4(b), for the Au@SiO_2 NPs dimer on a Au film, the large EM coupling is due to the "hot spots" transferred from the NP–NP gap to NP–surface gap, meanwhile, the more "hot spots" that occur, the stronger the EM coupling intensity that is obtained.

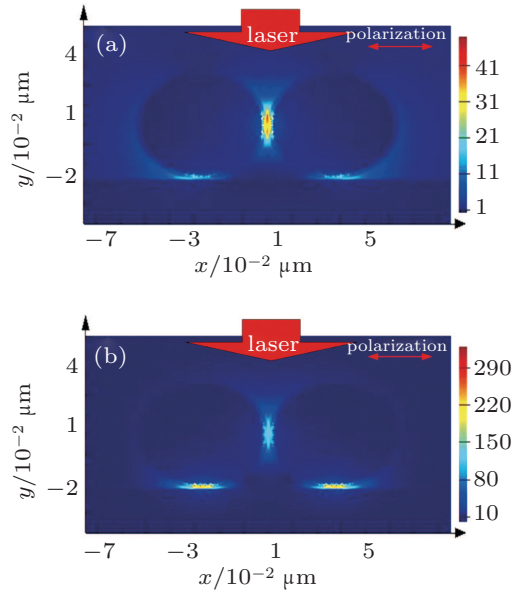


Fig. 4. (color online) FDTD simulations showing the EM field distributions of Au@SiO_2 dimers on gold film (a) and silicon substrate (b).

3.5. Effect of substrate on SERS signal

In order to verify the theoretical calculation and simulation accuracy, experimentally, the monolayer film of Au@SiO_2 NPs of ca. 50-nm diameter is transferred on the Au film and silicon substrate after rinsing with ethanol. The scanning electron microscopic images are shown in Figs. 5(a) and 5(b) and Fig. S2. Then the configuration is immersed in an ethanol solution containing R6G molecules. The Raman spectra (laser: 632.8 nm, 20 mW) are shown in Fig. 5(c), and we obtain SERS signal from the R6G molecules adsorbed in the gap between the NPs (b_1 and a_2 curves in Fig. 5(c)). It can be seen that the Raman enhancement properties of those two configurations are almost the same, showing that no matter what substrate is used, the EM coupling between the NP–NP gap still exists. Results show that experimental results are in good agreement with theoretical calculations. However, as can be seen in Fig. 4(b), for Au substrate, the EM coupling occurs not only in the NP–NP gap but also in the NP–surface gap. In order to further verify this simulation calculation, a Au@SiO_2 NPs monolayer film is transferred on the Au film and silicon substrate, separately. The Raman spectra are shown in Fig. 5(c), the SERS signals are only detected by molecules ad-

sorbed on the Au film surface (b_2 curve in Fig. 5(c)). But the signal intensity is much higher than that of the EM coupling between the NP–NP gaps. This can be well explained by the fact that if Au@SiO_2 NPs disperse on the silicon substrate, the EM coupling only occurs in "hot spots" in junctions between Au NPs. Due to the fact that the presence of a metal material will change the charge arrangement of NPs, the interaction between laser and dimer, the dipole occurs, and because the free electrons on the NP surface oscillate along the dimer axis, a large number of free electrons are focused on the interparticle spacing, resulting in a large amount of positive charge at the bottom of the NPs. Therefore, a number of electrons are induced on the gold film surface by electrostatic effect. Then, the redistribution of dipole will occur. Ultimately, the large EM coupling leads to the "hot spots" transferred from the NP–NP gaps to NP–surface gaps. In addition, the light which is reflected from the metal surface will increase the probability of resonance. This new type of coupling not only increases the EM coupling intensity, but also obtains more "hot spots". Meanwhile, this coupling mode has higher sensitivity and stability, higher ASEF than the coupling mode which occurs between Au NPs on silicon substrate (Figs. S6 and S7).

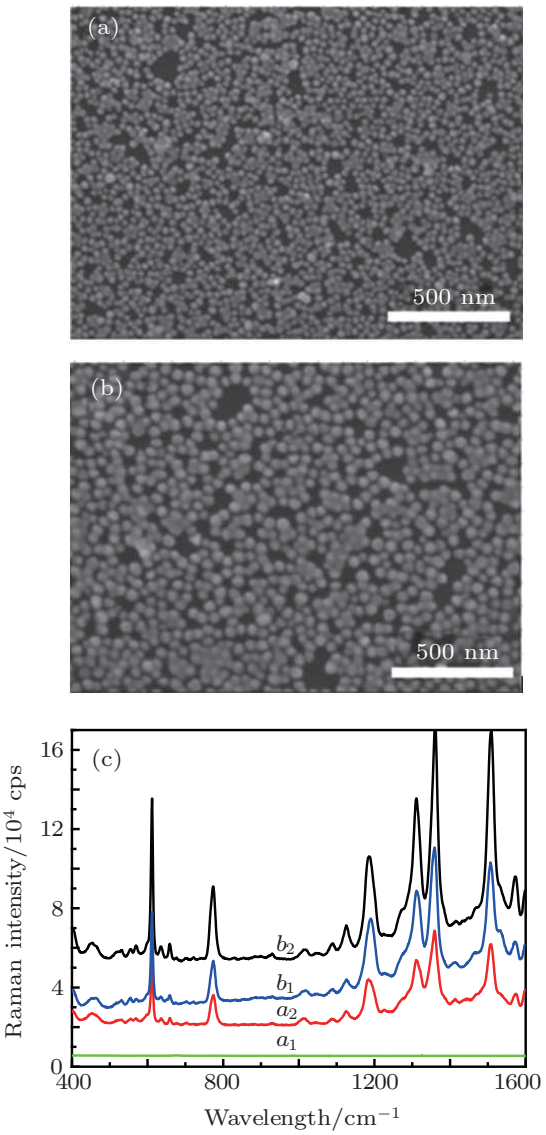


Fig. 5. (color online) SEM images of Au@SiO_2 NPs monolayer film on the silicon (a) and gold film (b). (c) Scheme for SERS detection with R6G molecules adsorbed in the gap between Au@SiO_2 NPs and Si (curve a_1), R6G molecules adsorbed in the gap between NPs (curve a_2), R6G molecules adsorbed in the gap between NPs (curve b_1), and R6G molecules adsorbed in the gap between NPs and Au film (curve b_2).

4. Conclusions and perspectives

In order to obtain the strongest electric field and much more "hot spots" in the metallic nanostructures, the FDTD method is used to simulate and calculate the EM field distribution in Au@SiO_2 NPs dimer on the different substrates. The calculation results show that on the silicon substrate, the bigger the particle size, the narrower the gap is and the stronger the EM field coupling intensity is. In addition, if the dimers disperse on the Au substrate, the signal comes from the gap region between the Au@SiO_2 NPs and the substrate instead of the gap between the dimers, and it has much more "hot spots" and high EFs. Experimentally, Au@SiO_2 NPs are prepared by using two methods, and Raman enhancements on different substrates are investigated. The FDTD calculation results fit well with the experimental data. Furthermore, we find that the signal intensity is determined not only by the NP size and the gap, but also by the position of the probe molecules in the "hot spots". The findings in this work can guide us in designing the metallic nanostructures to obtain a strongest field enhancement.

Appendix A: Supporting information

S1. Monolayer film of Au@SiO_2 NPs

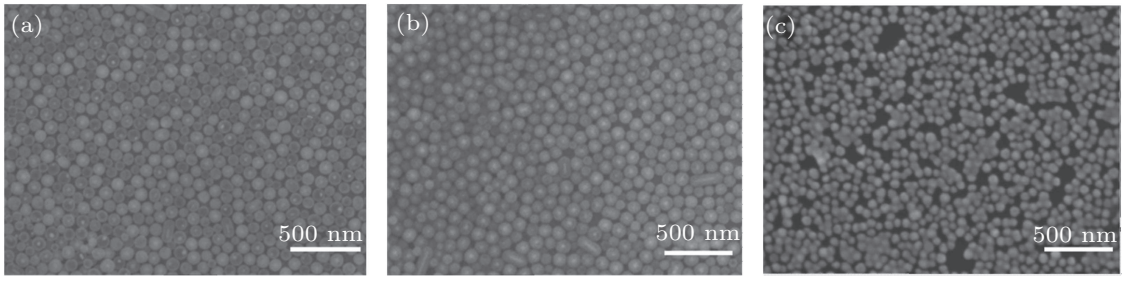


Fig. S1. SEM images of the monolayer films of Au@SiO_2 NPs with different shell thickness on silicon substrate: (a) 50 nm, (b) 35 nm, (c) 3 nm.

S2. Monolayer films of Au@SiO_2 NPs on gold film and silicon

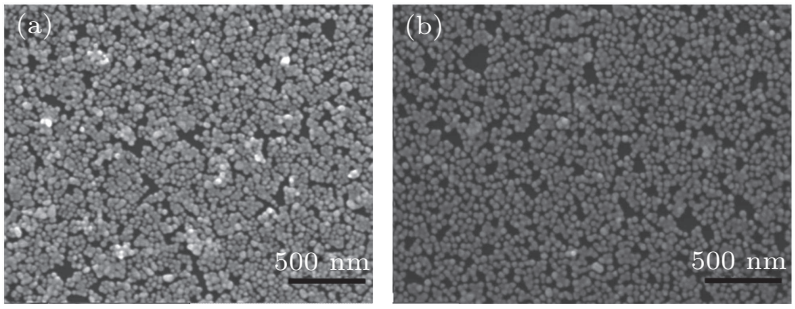


Fig. S2. Monolayer films of Au@SiO_2 NPs on gold film (a) and silicon (b).

S3. Simulation for same particle size with different gaps of Au NPs in air

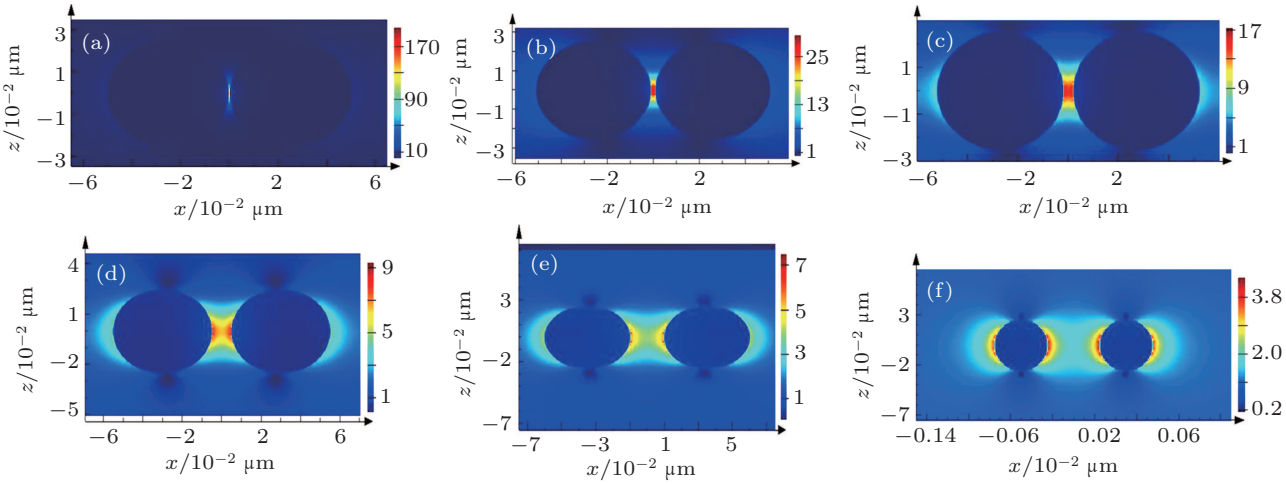


Fig. S3. (color online) 50-nm-diameter Au@SiO_2 NPs, and different gaps: (a) 1 nm, (b) 2 nm, (c) 4 nm, (d) 8 nm, (e) 30 nm, (f) 60 nm, where the laser polarization is parallel to the dimer axis and the laser wavelength is 633 nm.

S4. Simulation for same gap size with different nanoparticle of Au NPs in air

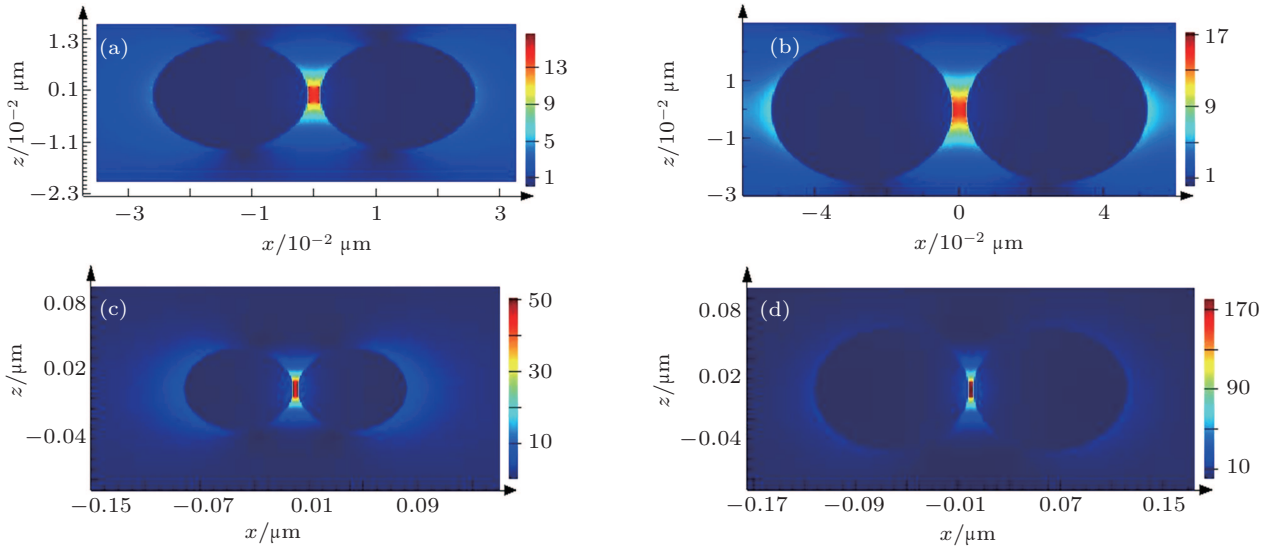


Fig. S4. (color online) 4-nm gap, different Au NPs sizes (a) 25 nm, (b) 50 nm, (c) 80 nm, (d) 120 nm, where the laser polarization is parallel to the dimer axis and the laser wavelength is 633 nm.

S5. Long tail effect

Ag@SiO_2 NPs instead of Au@SiO_2 NPs are prepared to study the long tail effect. Although the 50-nm silica shell is coated via the TEOS, the Raman signal of R6G still exists, and the NPs are evidently etched in H_2O_2 solution (Fig. S5(a)–S5(c)). These figures show that the pinholes exist in Ag@SiO_2 NPs. However, we acquire time-dependent SERS signals after mixing with

R6G (10^{-6} mol/L) to determine the effect of the pinhole. The enhancement signal does not change (Fig. S5(d)), which shows that the R6G molecule is larger than the pinhole. Furthermore, the SERS signal of R6G on the SiO_2 NPs (50 nm) disappears, which shows that a long tail effect occurs on the surface of the Au@SiO_2 NPs. Meanwhile, figures S5(e) and S5(f) show the remarkable stability of the Ag@SiO_2 NPs (shell-isolated) in H_2O_2 solution.

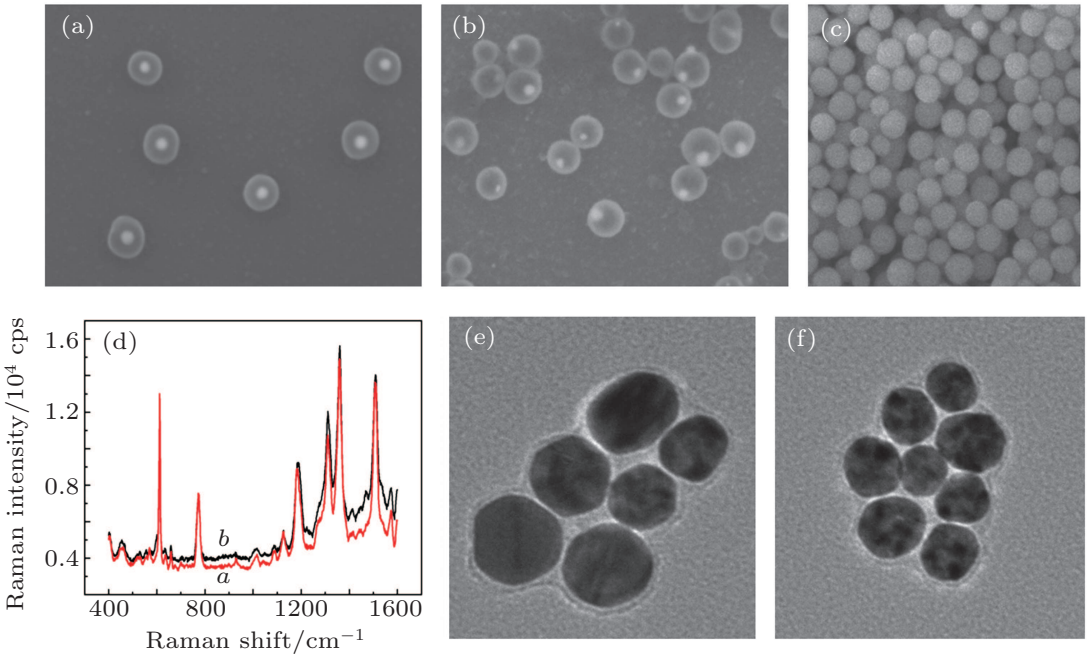
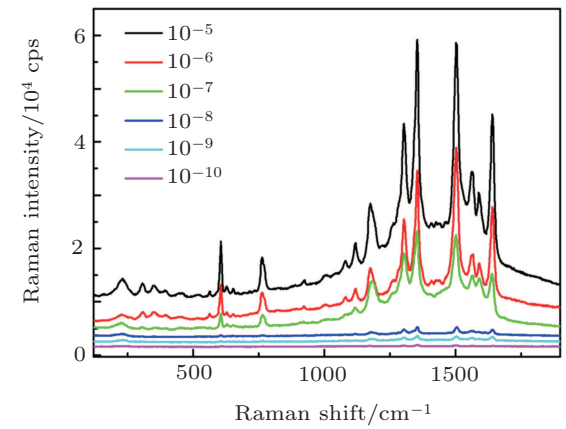


Fig. S5. (color online) Pinholes of Ag@SiO_2 NPs ((a)–(c)) and the pinhole-free Ag@SiO_2 NPs ((e), (f)), which are examined with a H_2O_2 solution; (d) Raman spectra of R6G molecule mixed with Au@SiO_2 NPs (50-nm shell thickness) at different times: (curve *a*) 10 min, (curve *b*) 1 h.

S6. High sensitivity, high average enhancement factor



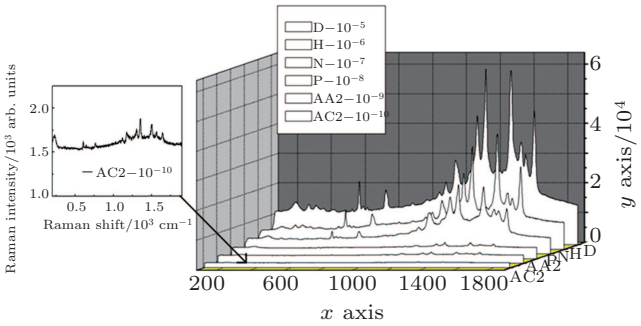


Fig. S6. (color online) SERS spectra of different concentrations of R6G on the monolayer films of Au@SiO_2 NPs (D) 10^{-5} M, (H) 10^{-6} M, (N) 10^{-7} M, (P) 10^{-8} M, (AA2) 10^{-9} M, and (AC2) 10^{-10} M.

S7. High reproducibility

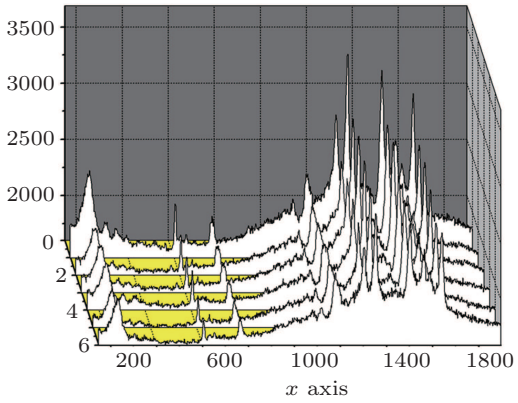


Fig. S7. (color online) SERS spectra of R6G (10^{-8} mol/L) deposited on monolayer film of Au@SiO_2 NPs.

Acknowledgment

The authors would like to thank Professor J H Han and Professor G H Yang for assistance in theory and helpful discussion.

References

[1] Fleischman M, Hendra P J and McQuilla A 1974 *J. Chem. Phys. Lett.* **26** 163

[2] Quyen T T B, Su W N, Chen K J, Pan C J, Rick J, Chang C C and Hwang B J 2013 *Journal of Raman Spectroscopy* **44** 1671

[3] Zheng X G, Guo Q X and Meng D D 2011 *Chin. Phys. Lett.* **28** 087805

[4] Wang X F, Xing X, Zhang Q L, You J L, Wu J, Zhang D M, Sun Y, Sun D L and Yin S T 2015 *Chin. Phys. B* **24** 098104
[5] Tian Z Q, Ren B and Wu D Y 2002 *J. Phys. Chem. B* **106** 9463
[6] Li M S and Yang C X 2010 *Chin. Phys. Lett.* **27** 044202
[7] Lee S J, Guan Z, Xu H and Moskovits M 2007 *J. Phys. Chem. C* **111** 17985
[8] Zhong Y T, Cheng Z Q and Ma L 2014 *Chin. Phys. Lett.* **31** 047302
[9] Wu D Y, Li J F, Ren B and Tian Z Q 2008 *Chem. Soc. Rev.* **37** 1025
[10] Park W H and Kim Z H 2010 *Nano Lett.* **10** 4040
[11] Pettinger B, Picardi G, Schuster R and Ertl G 2000 *Electrochemistry* **68** 942
[12] Chen L, Liu F X and Zhan P 2011 *Chin. Phys. Lett.* **28** 057801
[13] Cheng L, Ma C S and Yang G 2014 *J. Mater. Chem. A* **2** 4534
[14] Zhuang M D, Liu Z, Ren B and Tian Z Q 2010 *Sci. China: Chem.* **53** 426
[15] Liu Z, Zhang F L, Yang Z B, *et al.* 2013 *J. Mater. Chem. C* **1** 5567
[16] Li J F, Huang Y F, Ding Y, Yang Z L, Li S B, Zhou X S and Tian Z Q 2010 *Nature* **464** 392
[17] Li J F, Ding S Y, Yang Z L, Bai M L, Anema J R, Wang X, Wang A, Wu D Y, Ren B, Hou S M, Wandlowski T and Tian Z Q 2011 *J. Am. Chem. Soc.* **133** 15922
[18] Li J F, Zhang Y J, Rudnev A V, Anema J R, Li S B, Hong W J, Panneerselvam R, Lipkowski J, Wandlowski T and Tian Z Q 2015 *J. Am. Chem. Soc.* **137** 2400
[19] Yang Z B, Zhang L and You H J 2014 *Part. Part. Syst. Charact.* **31** 390
[20] Knight M W, Wu Y P, Lassiter J B, Nordlander P and Halas N J 2009 *Nano Lett.* **9** 2188
[21] Frens G 1973 *Nat. Phys. Sci.* **241** 20
[22] Stober W, Fink A and Born E 1968 *J. Colloid Interface Sci.* **26** 62
[23] Li Y J, Huang W J and Sun S G 2006 *Angew. Chem. Int. Ed.* **45** 2537
[24] Wang X, Li M H, Meng L Y, Lin K Q, Feng J M, Huang T X, Yang Z L and Ren B 2014 *ACS Nano* **8** 528